Numerical Simulation of Pulsed Electromagnetic Stamping Processes.

N. Bessonov[1], S. Golovashchenko[2]

[1] Institute of the Problems of Mechanical Engineering, Russian Academy of Sciences, St. Petersburg, Russia

[2] Manufacturing & Processes Department, Ford Research & Advanced Engineering, Dearborn, USA

Abstract

In earlier published papers simulation of electromagnetic forming (EMF) was often conducted assuming that pulsed electromagnetic load can be replaced by the pulse of mechanical force calculating its parameters similar to R-L-C electric circuit. However, in many practical cases, parameters of this circuit are variable during the process because of the displacement of the blank and from one operation to another due to the accumulation of heat in the coil. The distribution of electromagnetic forces is also non-uniform and may affect the quality of the part being stamped. In our opinion, the accuracy of the simulation of EMF can be significantly improved if the formulation of the problem includes Maxwell equations of the electromagnetic field propagation, equations of dynamic elastic-plastic deformation, and heat transfer equations all coupled together. In addition, this approach may provide knowledge of electromagnetic coil deformation, which was investigated earlier with significant simplifications. The complexity of the problem is defined by mutual dependence of all three physical processes (electromagnetic field propagation, dynamic elastic-plastic deformation, and heat transfer) and variable boundary conditions.

The propagation of the electromagnetic field is defined by quasi-stationary Maxwell equations transformed in Lagrangian form. The dynamics of elastic-plastic deformation is modeled using the solid mechanics equation of motion, the modified theory of elastic plastic flow, and the Von Mises yield criterion. The energy conservation law is employed for the simulation of heat transfer, which is important to define the appropriate stamping rate without overheating the coil.

The developed methodology is illustrated by 2D examples of cone formation from sheet using a flat coil and the conical die and 2D plane strain sheet formation by direct propagation of the electric current through the metal bar, serving as a coil, and through the deformed sheet.

Keywords:

Forming, Sheet, High Strain-Rate

1 Introduction

In earlier published papers simulation of electromagnetic forming (EMF) was often conducted assuming that pulsed electromagnetic load can be replaced by the pulse of mechanical force [1]. Parameters of this pulse were calculated similar to R-L-C electric circuit [2]. However, in many practical cases, parameters of this circuit are variable through the process because of the displacement of the blank and from one operation to another due to the accumulation of heat in the coil. The distribution of electromagnetic forces is also non-uniform and may affect the quality of the part being stamped. In our opinion, the accuracy of the simulation of EMF can be significantly improved if the formulation of the problem includes Maxwell equations of the electromagnetic field propagation, equations of dynamic elastic-plastic deformation, and heat transfer equations all coupled together. In addition, this approach may provide knowledge of the deformation of the electromagnetic coil, which was investigated earlier with significant simplifications [3].
The complexity of the problem is defined by mutual dependence of all three physical processes (electromagnetic field propagation, dynamic elastic-plastic deformation, and heat transfer) and variable boundary conditions.

2 Theoretical approach

The propagation of the electromagnetic field is defined by quasi-stationary Maxwell equations:

$$\nabla \times H = j \tag{1}$$

$$\mu_a \frac{\partial H}{\partial t} = -\nabla \times E \tag{2}$$

$$j = \sigma \cdot (E + \mu_a v \times H) \tag{3}$$

where H is the magnetic field intensity; j is the current density; E is the electric field intensity; σ is the electric conductivity; v is the velocity; μ_a is the magnetic permeability of medium under consideration. For short duration processes we assume $\mu_a = 4\pi 10^{-7}$ H/m.

Taking into account specifics of the electromagnetic forming processes, including an almost stationary coil, a die and a quickly accelerated blank, the equation for the magnetic field intensity H can be transformed in Lagrangian form. Based upon equations (1)-(3), the equation relating to the vector H can be written as:

$$\mu_a \frac{\partial H}{\partial t} = -\nabla \times \left(\frac{1}{\sigma} \nabla \times H - \mu_a v \times H \right) \tag{4}$$

or transformed in integral form

$$\mu_a \frac{d}{dt} \int_V H dV - \mu_a \oint_S v H ds = \oint_S \frac{1}{\sigma} ds \times (\nabla \times H) \tag{5}$$

Where V is the volume restricted by the surface s; $ds = ndS$; n is external normal to S; $d/dt = \partial/\partial t + v \cdot \nabla$.
Dynamic elastic-plastic deformation of solids can be defined by the following equations:

$$\rho \frac{d}{dt} \int_V v dV = \int_S \sigma \cdot ds + \int_V f dV \tag{6}$$

where

$$f = j \times B = -\mu_a H \times j = -\mu_a H \times (\nabla \times H) \tag{7}$$

$\sigma = pI + S$ is the stress tensor; ρ is the density; p is the pressure; S is the deviator part of the stress tensor,

$$p = K\left(\frac{V}{V_0} - 1\right), \; S = GB_D \tag{8}$$

V and V_0 are actual and original volumes respectively; B_D is the deviator part of the left Cauchy-Green tensor B; $B = F \cdot F^T$; $F = dx/dX$ is the deformation gradient tensor; x is the vector of actual location; X is the vector of original location; K and G are bulk and shear modulus respectively.
The Von Mises yield criterion is used to describe the elastic limit:

$$-J_2(S) \le \frac{\sigma_y^2}{3} \tag{9}$$

where σ_y is the current plastic flow stress (depends upon strain and strain rate).
The energy conservation law is employed in the following form:

$$\frac{d}{dt} \int_V c_V T dV = \int_V P dV \tag{10}$$

where T is the temperature; $P = j^2/\sigma$ is the power generated in the form of heat while the electric current is running through the coil and blank because of the active resistance of their materials.

The system of equations (5)-(10) represents the full formulation of the problem. This system is solved numerically using the finite volume method. Initially, the nonorthogonal Lagrangian mesh is introduced; a fragment of the 2D mesh (for simplicity) is shown in Figure 1(a). The computational domain is divided into cells. Each cell consists of two triangles in 2D case called elements (or six tetrahedrons in 3D case) as illustrated in Figure 1(b) and (c) respectively.

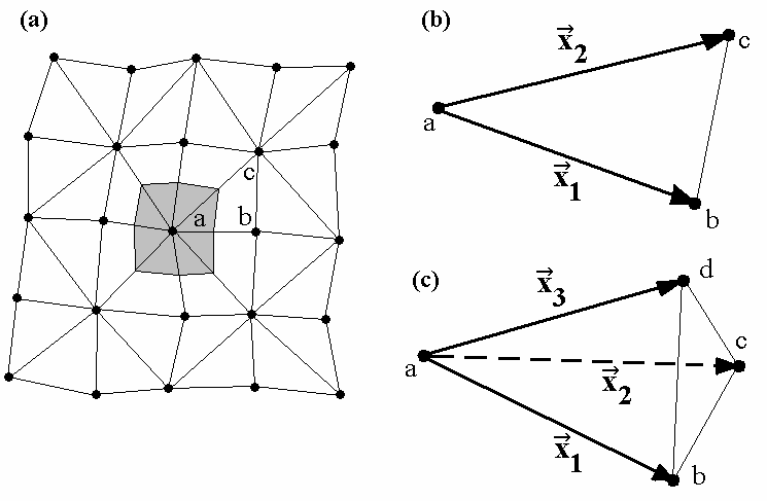

Figure 1: *(a) Fragment of 2D Lagrangian mesh (• are the nodes); (b) 2D element; (c) 3D element*

A control volume *V* (grey in Figure 1(a)) is corresponded to every node of the mesh. The explicit approximation is used for the calculation of new values of velocity in every node. Equations (5), (6) and (10) are solved using the technique described in [4].

For the solution of the elastic-plastic part of the problem (6)-(9) the new return-map algorithm was applied. Taking into account the equations (8), we can transform the condition (9) in the form

$$-J_2(B_D) \le \frac{\sigma_y^2}{3G^2} \equiv k^2 \tag{11}$$

where k^2 is a material characteristic. The condition (11) determines the restrictions on the deformation field. We will illustrate all the specifics of the new return-map algorithm considering only one tetrahedral element of the mesh *abcd* (Figure 1(c)). We denote the initial position of the tetrahedron vertices at the initial time by position-vectors X_a, X_b, X_c and X_d. Due to the deformation process, the vertices shift from their initial positions. We denote the actual position of the vertices of the tetrahedral element at time *t* by x_a, x_b, x_c and x_d. Let x_i and X_i (i = 1,2,3) be the right-hand set of vectors directed along any three different ribs of the tetrahedron (Figure 1(c)). Let us introduce the linear transformation of the element from its initial to its actual position (see more details in [4]):

$$x = A \cdot X + b \tag{12}$$

Using the transformation (12) we can find the deformation gradient tensor *F* in the element

$$F = \frac{dx}{dX} = \frac{\partial(A_{ik}X_k + b_i)}{\partial X_m} e_i e_m = A_{ik}\delta_{km} e_i e_m = A \tag{13}$$

We define *A* from the following system

$$\begin{aligned} x_1 &= A \cdot X_1 \\ x_2 &= A \cdot X_2 \\ x_3 &= A \cdot X_3 \end{aligned} \tag{14}$$

Then we obtain

$$A = x_i e_i \cdot (X_m e_i) \tag{15}$$

Finally, combining (13) and (15) we can define the finite difference approximation of B for the element:

$$B = R^T \cdot G \cdot R \tag{16}$$

where $G = e_k\, X^k \cdot X^m\, e_m$; $R = e_k\, x_k$; x^i and X^i are the sets of vectors reciprocal with x_i and X_i respectively (see for example [4]).
It is important to stress that all information about the initial configuration of the element is concentrated in tensor G and its initial volume V_0. We can assert that G and V_0 play the role of the memory of the element and keep the information about its initial configuration. Among two G and V_0, the condition (11) contains G only. We named it the tensor of initial configuration. If the deformation of the element exceeds the critical value, then condition (11) is not satisfied any more and the internal structure of the solid body is irreversibly changed. In other words, the initial configuration of the element and, consequently, the tensor G should be changed in such a way that the equation

$$-J_2(B_D) = k^2 \tag{17}$$

is satisfied.
We proceed step by step in time. At the initial time step in addition to all other values, we have to calculate G for every element of the mesh. Assuming that we had already found the new positions of the element vertices and then calculated the set of vectors $x_s{}^{n+1}$ at n + 1 time step, we carry out the predictor step and put

$$B' = \left(R^T\right)^{n+1} \cdot G^n \cdot R^{n+1} \tag{18}$$

If the condition

$$-J_2(B'_D) \le k^2 \tag{19}$$

is satisfied, then the tensor G^n does not change (i.e. $G^{n+1} = G^n$). Suppose that condition (19) does not hold. Then we should find the new tensor G^{n+1} for the element which satisfies the following equation for $B^{n+1} = (R^T)^{n+1} \cdot G^{n+1} R^{n+1}$:

$$-J_2\left(B_D^{n+1}\right) = k^2 \tag{20}$$

The value of G^{n+1} satisfying this condition may be defined in the form

$$G^{n+1} = aG^n + (1-a) \cdot G'^{n+1} \tag{21}$$

where $G' = e_k\, x^k \cdot x^m\, e_m$ and

$$a = \frac{k}{\sqrt{-J_2(B'_D)}} \tag{22}$$

Now equation (20) is satisfied exactly.
The “difference” (difference - not in a sense of withholding, but in a sense of shape difference) between G^{n+1} and G' is a critical elastic deformation of the element permissible by

the condition (19). The difference between G^{n+1} and G^{n} configurations is the plastic (irreversible) deformation.

3 Numerical examples

The described algorithm was employed for simulation of pulsed electromagnetic forming of aluminium sheet into a conical die cavity. The five-turn flat electromagnetic coil was used as a tool generating the electromagnetic pressure, as shown in Figure 3. The distribution of the electromagnetic field was defined in a 2D formulation assuming that the coil is axisymmetrical and includes five circular turns.

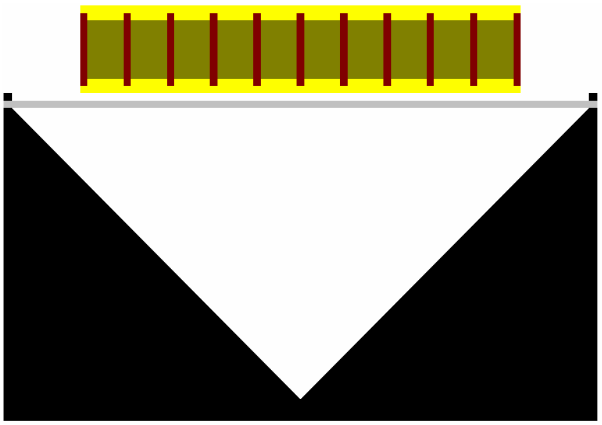

Figure 3: *Assumed 2D schematic of the process*

The electromagnetic forming machine serving as a generator of pulsed currents can be represented as a R-L-C circuit, as it is indicated in Figure 4. The electric current running into a coil-blank system as a boundary condition can be defined using an explicit integration procedure.

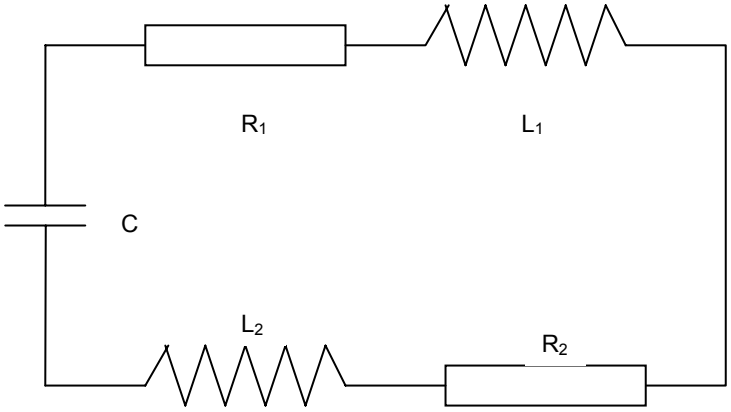

Figure 4: *R-L-C contour: R_1, L_1 and C are the characteristics of the electromagnetic forming machine; R_2 and L_2 are the characteristics of the coil*

The full electric current in this circuit can be defined from the following system:

$$\frac{d(LI)}{dt} + RI = U \tag{23}$$

$$C\frac{dU}{dt} = -I \tag{24}$$

where $L = L_1 + L_2$ and $R = R_1 + R_2$.
At every time step we solved equations (23) and (24) and, based upon the defined value of the current I, calculated the density of the electric current in the coil $j = I/S$, where S is the square of the cross-section of the coil.

Characteristics of the electromagnetic forming machine, serving as an external circuit to the coil-blank system, were the following: R_1 = 0.01…0.001 Ω; $L_1 = 10^{-9}$ H; $C = 2 \cdot 10^{-4}$ F; The charging voltage of the capacitor bank was U_0 = 5 kV. The values of R_2 and L_2 were defined at every time integration step.

The contact interaction between the blank and the die was modeled employing the mild contact algorithm. The whole problem was solved numerically using a Lagrangian mesh which was periodically re-meshed in the areas between the coil and the blank and between the blank and the die. The results of the simulation of a 1 mm aluminum sheet formation into a conical die cavity is shown in Figures 5 and 6. It can be indicated that the central part of the sheet is delayed relatively to the area adjacent to it. The transverse wave of plastic deformation propagates in radial direction from the periphery of the blank towards its center, as it was previously observed in experimental studies [6].

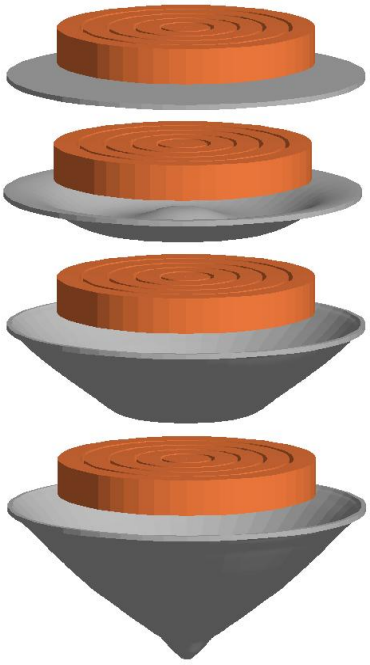

Figure 5: *Dynamics of forming of an aluminium sheet into a conical die*

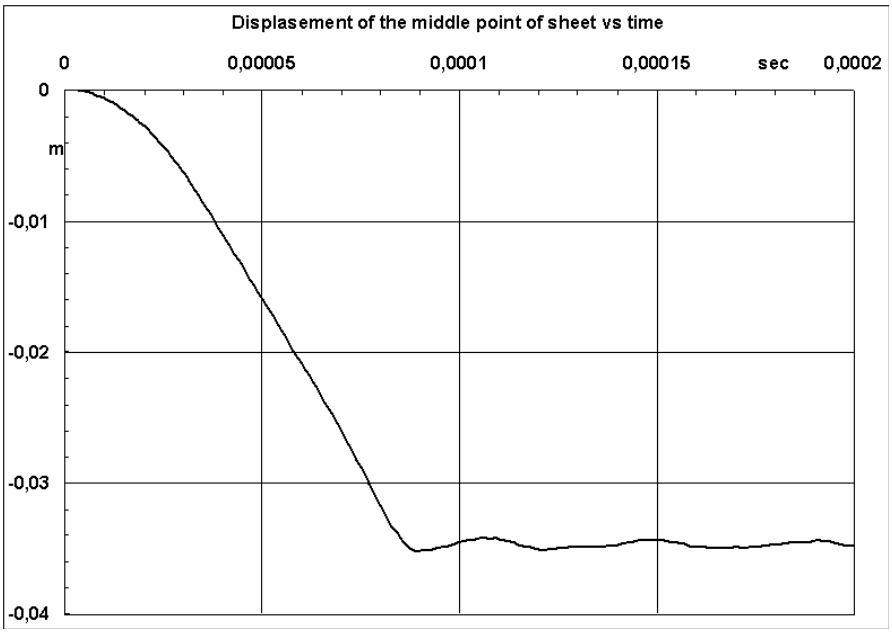

Figure 6: *Displacement of the middle point of the sheet vs time*

The distribution of the electromagnetic field intensity in transverse pulsed forming of sheets by direct propagation of the electric current through the metal bar, serving as a coil, and in opposite direction through the deformed aluminium sheet is shown in Figure 7. This test shows the important benefit of providing an almost uniform distribution of electromagnetic pulsed pressure on the sample. The corresponding formation of the 100 mm long and 1 mm thick aluminium strip is illustrated in Figure 8.

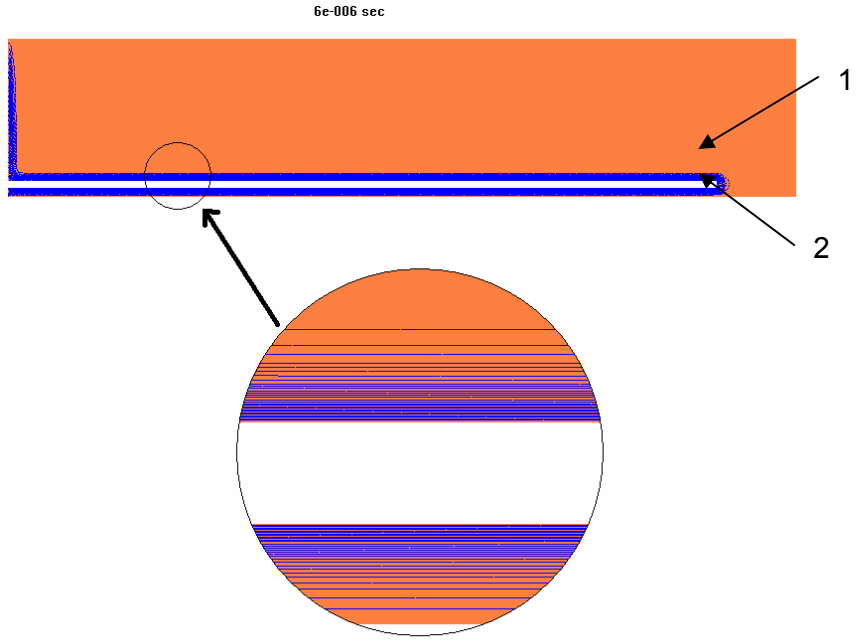

Figure 7: *Distribution of the electromagnetic field intensity for the 2D plane strain sheet formation by direct propagation of the electric current through the metal bar 1, serving as a coil, and through the deformed aluminium sheet 2*

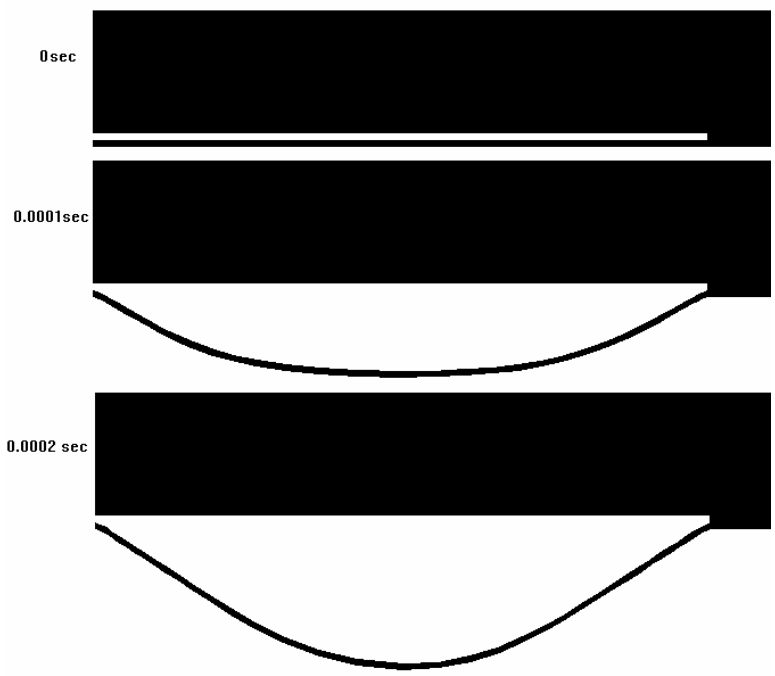

Figure 8: *Deformation process for the strip subjected to pulsed electromagnetic load by direct current propagation*

4 Conclusions

A fully coupled numerical procedure incorporating an electromagnetic field propagation, a dynamic elastic-plastic deformation, and a heat transfer has been developed based on the Finite Volume Method of integration. Provided examples validate the developed model for plane strain and axisymmetrical deformation.

References

[1] *Golovashchenko, S.; Bessonov, N.:* Numerical Simulation of High-Rate Stamping of Tubes and Sheets, CRM Proceedings and Lecture Notes. American Mathematical Society, Volume 21, 1999, p.199-207.

[2] *Beliy, I.; Fertik, S.; Chimenko, L.:* Reference book on magnetic-pulsed stamping, Charkov, USSR, 1976, 167p.

[3] *Golovashchenko, S.; Shutov, R.:* Numerical modeling of dynamics of deformation of multi-turn cylindrical coil for electromagnetic forming. Proceedings of High Educational Institutions. Ser. Mechanical Engineering, N 10, 1994, p.123-128 (in Russian).

[4] *Bessonov, N.; Song, D.:* Application of vector calculus to numerical simulation of continuum mechanics problems. Journal of Computational Physics. 167/1,1999, p.22-38.

[5] *Bessonov, N.; Golovashchenko S.:* New algorithm of simulation of elastic-plastic deformation based on updated initial configuration of solid body (In print).

[6] *Legchilin, A.:* Study of the stamping process using pulsed electromagnetic field. PhD Dissertation, Bauman Moscow High Technical School, Russia, 1969, 282p.